Food Chemistry 119 (2010) 896–902

Contents lists available at ScienceDirect

Food Chemistry

journal homepage: www.elsevier.com/locate/foodchem

Nano/sub-microsized lignan glycosides from sesame meal exhibit higher transport and absorption efficiency in Caco-2 cell monolayer

Chia-Ding Liao [a], Wei-Lun Hung [a], Kuo-Ching Jan [a], An-I Yeh [a], Chi-Tang Ho [a,b], Lucy Sun Hwang [a,*]

[a] Graduate Institute of Food Science and Technology, National Taiwan University, Taipei 106, Taiwan
[b] Department of Food Science, Rutgers University, 65 Dudley Road, New Brunswick, New Jersey 08901, USA

ARTICLE INFO

Article history:
Received 4 June 2009
Received in revised form 3 July 2009
Accepted 22 July 2009

Keywords:
Lignan glycoside
Sesame meal
Transport
Absorption
Nanotechnology
Caco-2 cell monolayer

ABSTRACT

In the present study, we investigated whether lignan glycosides from sesame meal (LGSM), after nano/sub-microsizing, will exhibit higher transport and absorption efficiencies than LGSM. The average particle size of 1% LGSM aqueous suspension reduced from approximately 2 μm–200 nm after media-milling with zirconia beads. The transport and absorption of LGSM and nano/sub-microsized LGSM (N-LGSM) using Caco-2 human epithelial colorectal adenocarcinoma cells, a model simulating human intestinal absorption was examined. The permeability of sesaminol triglucoside (ST) in N-LGSM and LGSM was 1.41 ± 0.16 and 1.07 ± 0.21 (10^{-6} cm/s), respectively, indicating that ST in N-LGSM was more efficiently transported through the monolayer. In addition, N-LGSM exhibited 35.7% higher absorption efficiency than LGSM. The better performance of N-LGSM may be attributed to the (a) smaller particle size and larger surface area; (b) increased mucosal permeability, and (c) improved intestinal absorption due to the formation of nanoemulsion droplets.

1. Introduction

Sesame (*Sesamum indicum* L.) has long been categorised as one of the traditional functional foods in East Asian countries. Sesame seed, composed of 50% lipid and 20% protein, is one of the most important oilseed crops in the world (Namiki, 1995; Shyu & Hwang, 2002). Lignans and lignan glycosides are important functional components in sesame. The major sesame lignans are sesamin and sesamolin, which are found in sesame oil. Lignan glycosides, which exist mainly in defatted sesame meal, are hydrophilic antioxidants. The major lignan glycosides present in sesame are sesaminol glucosides, pinoresinol glucosides and sesamolinol glucosides (Katsuzaki, Kawakishi, & Osawa, 1994). Several biological effects of these lignan glycosides have been studied. Defatted sesame flour containing 1% sesaminol glucoside has been reported to decrease susceptibility to oxidative stress in hypercholesteroelemic rabbits (Kang, Kawai, Naito, & Osawa, 1999). Sesaminol glucosides showed a protective effect on beta-amyloid (Aβ)-induced neuronal cell death (Lee, Ha, Son, Kim, & Hong, 2005). In addition, sesaminol glucosides have been shown to be potential anticancer agents (Sheng et al., 2007). As a by-product, sesame meal would be of added value if it could be used in the food industry.

Nanotechnology has recently captured the attention of researchers, manufactures and the general population. Due to the advantage of size effect and high surface reactivity of nanoparticles, nanotechnology is already used in pharmaceutical applications to increasing the bioavailability of drugs (Jia, Wong, Cerna, & Weitman, 2002; Jia, Wong, Wang, Garza, & Weitman, 2003). However, there are few reports on applications of nanotechnology in foods. The advantages and limitations of its use in the food industry are not yet fully understood. Several techniques have been applied to produce food nanosuspensions, such as media-milling and high pressure homogenisation (Gao et al., 2008; Jia et al., 2003). The specific physico-chemical properties at the nanoscale are expected to result in increased reactivity with biological systems. Wet-milling technology using Yttria-stabilised zirconia beads as a milling medium has been used to formulate physically stable red mould rice dispersions (Yu, Lee, & Pan, 2006). Similarly, ketoconazole nanoparticles were also prepared using a media-milling technique with Yttria-stabilised zirconia beads (Basa, 2008). However, more information on the absorption, distribution, metabolism and excretion of food nanoparticles is needed.

Caco-2 human colon epithelial colorectal adenocarcinoma cells were chosen as a model for this study. When allowed to differentiate, Caco-2 cells exhibit morphology and express many of the hydrolytic enzymes present in the small intestinal brush border (Artursson, 1990; Walgren, Walle, & Walle, 1998). This *in vitro* model has been widely used to investigate cell transport and absorption of phytochemicals such as anthocyanins, quercetin, quercetin glucosides and flavone (Boyer, Brown, & Liu, 2004; Kobayashi & Konishi, 2008; Yi, Akoh, Fischer, & Krewer, 2006).

* Corresponding author. Tel.: +886 2 23629984; fax: +886 2 33664113.
E-mail address: lshwang@ntu.edu.tw (L.S. Hwang).

0308-8146/$ - see front matter © 2009 Elsevier Ltd. All rights reserved.
doi:10.1016/j.foodchem.2009.07.056

According to the literature, permeability coefficients determined by the Caco-2 cell monolayer have been shown to correlate highly with human absorption *in vivo* (Foger, Kopf, Loretz, Albrecht, & Bernkop-Schnurch, 2007; Lau et al., 2004).

Many reports have shown that the smaller the particle size, the higher the absorption efficiency in a Caco-2 cell model. The size-dependent permeability and bioavailability of an inhibitor of bovine viral diarrhaea virus (301029) was reported by Jia et al. (2002). It showed a good correlation between *in vitro* Caco-2 cell and *in vivo* oral absorption of the drug. The faster absorption of 301029 after nanonization is likely due to increases in dissolution rate and saturation solubility of the drug, as well as an increased adhesiveness of nanoparticles to intestinal mucosa. An increase in adhesion surface area between nanoparticles and the mucin layer coating intestinal epithelium of villi facilitates the nanosized drug to traverse the mucin layer and the epithelial cells.

The predictive usefulness of the Caco-2 model has been tested by comparing the AUC with the *in vivo* oral bioavailability reported. Linear regression analysis showed a reasonable correlation ($R^2 = 0.86$) between the *in vitro* AUC and *in vivo* oral bioavailability. *In vitro* permeability across Caco-2 monolayer and *in vivo* oral bioavailability in rats and human was reported (Foger et al., 2007). A good correlation between the two systems was also observed (Yee, 1997).

In this study, we obtained nano/sub-microsized lignan glycosides from sesame meal (LGSM) by wet-milling. The objectives of the experiments were (1) to use the Caco-2 cell monolayer model to evaluate the transport and absorption of sesaminol triglucoside (ST) and (2) to determine whether the transport and absorption efficiency of N-LGSM differs from LGSM.

2. Materials and methods

2.1. Materials and chemicals

Black sesame meal was supplied by Yuan-Shun Food Co. (Yun-Ling County, Taiwan). Sesaminol triglucoside (ST) standard (purity = 99%, identified by Nuclear Magnetic Resonance spectroscopy) was extracted and purified from sesame meal using a method reported in the literature (Katsuzaki et al., 1994). In brief, the sesame meal was defatted with *n*-hexane and extracted with 80% methanol. The 80% methanol extract was charged into an Amberlite XAD-2 column, which was prepared from Amberlite XAD resin (20–60 mesh, Rohm and Haas Co., Philadelphia, PA, USA), and eluted with H_2O, 20% methanol, 40% methanol and 60% methanol. The 60% methanol fraction was then purified by preparative HPLC under the following conditions: column Cosmosil ODS (250 × 20 mm i.d., Nacalai Tesque, Kyoto, Japan), solvent methanol, flow rate 4 mL/min. The chemical structure of ST is shown in Fig. 1.

Methanol (purity = 99.5%, HPLC grade) and *n*-hexane (purity = 98%) were purchased from Merck Co. (Darmstadt, Germany) and Tedia Co. (Fairfield, OH, USA), respectively. Deionised water (Millipore Co., Bedford, MA, USA) was used for all preparations.

2.2. Preparation of the crude extract of lignan glycosides

The method was adapted from Shyu and Hwang (2002). Black sesame meal was extracted with *n*-hexane (1:10, g/mL) by stirring for 8 h at room temperature (2 times). After removal of supernatant, the defatted sesame meal was collected and then extracted with 80% methanol (1:10, g/mL) by stirring for 8 h at room temperature (2 times). This methanol extract was desolventized under reduced pressure to afford the crude extract of lignan glycosides from sesame meal (LGSM) for the following experiments.

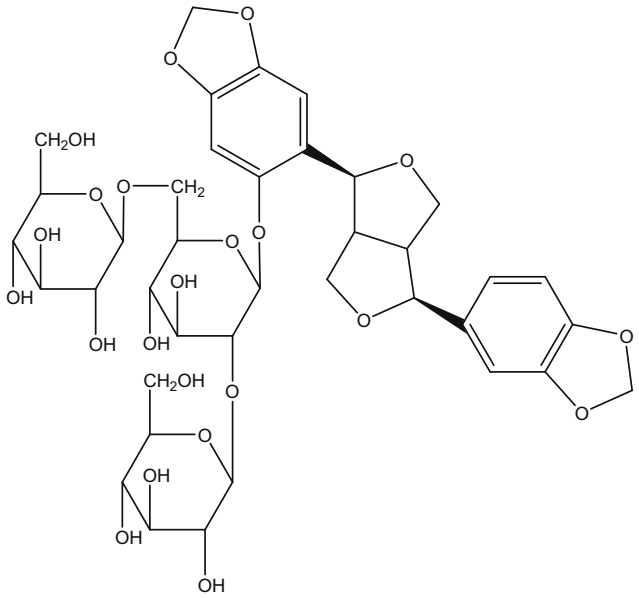

Fig. 1. Chemical structure of sesaminol triglucoside.

2.3. Preparation of nano/sub-microsuspension of lignan glycosides from sesame meal

Nano/sub-microsized LGSM was produced using a wet-milling process in a milling machine (MiniPur, Netzsch-Feinmahltechnik GmbH, Staufen, Germany). Milling was performed using Yttria-stabilised zirconia beads with a diameter of 0.3 mm. Effective particle size reduction was achieved under following conditions: Four grams of LGSM, the crude extract of lignan glycosides, were suspended in 400 mL of deionised water. Feed speed was 360 mL/min. The effects of rotation speed (600, 1800 and 3600 rpm) and milling time (5, 10, 30, 60 and 90 min) on size distribution were investigated. The suspension was agitated and recycled in the milling system by a pump. The bulk volume of milling medium was 140 mL. The milling temperature was controlled by a cooler with temperature set at 10 °C. Finally, the nano/sub-microsized LGSM suspension (N-LGSM) was collected for particle size determination.

2.4. Particle size and morphology determination

The particle size of N-LGSM was determined by both dynamic light scattering and transmission electron microscopy (TEM). Dynamic light scattering measurements were performed using a light scattering particle size analyser (Nanotrac 150, Microtrac Inc., Largo, FL, USA). In order to eliminate air bubbles in suspension just after milling, samples were degassed by a sonicator (Model 3510, Branson Ultrasonic Co., Danbury, CT, USA) at a frequency of 40 kHz for 10 min prior to particle size measurement. The particle size distribution and average particle size were obtained after analysing. In addition, the size and morphology of N-LGSM was studied by TEM (Model JSM-1200EX II, JEOL, Tokyo, Japan). Ten microlitres of N-LGSM was added to 200 mesh carbon-coated copper grids (Electron Microspray Science, Hatfield, PA, USA) and the excess liquid was drained off with a Whatman filter paper. Copper grids containing the sample as a dry film was placed on a TEM sample holder and observed at an accelerating voltage of 80 kV. A Sudan stain test was also performed using a 0.2% Sudan III (Sigma–Aldrich, St. Louis, MO, USA) solution in 70% ethanol. After adding 5 mL of N-LGSM suspension in a clean tube, 0.5 mL of Sudan III solution was added and mixed well by a vortexer for 2 min. Twenty microlitres of Sudan III stained sample was added to the micro-

scopic slide and observed using a Leica DM6000B optical microscope (Leica Microsystems, Wetzlar, Germany).

2.5. Caco-2 cell cultures

Passage 18 Caco-2 cells, obtained from American Type Culture Collection, were cultured in Dulbecco's modified Eagle's medium (DMEM; GIBCO, Carlsbad, CA, USA), supplemented with 10% foetal bovine serum (GIBCO), 1% nonessential amino acid solution and antibiotics (100 U/mL penicillin and 100 μg/mL streptomycin, GIBCO). Cells were grown in an incubator with 5% CO_2 and 95% humidity at 37 °C. Growth medium was changed every 2–3 d. Cells from passage 25–35 were used in the experiments.

Transwell inserts (polycarbonate membrane, diameter of 1.2 cm and pore size of 0.4 μm, Corning Costar Co., Corning, NY, USA) in 12 well plates were used. Caco-2 cells were seeded on the membrane inserts at a density of 5×10^5 cells/cm^2. The apical and basolateral sides contained 0.5 and 1.5 mL of culture medium, respectively. Medium was replaced 3 times per week. The Caco-2 cells used in the experiments were about 21 days postseeding in the Transwells. The integrity of the cell layer was evaluated by measuring the transepithelial electrical resistance (TEER) values with Millicell-ERS equipment (Millipore Co., Bedford, MA, USA). Monolayers with the TEER values >400 Ω cm^2 were selected for transport and absorption experiments.

2.6. Transport experiments

The transport study was performed according to the methods reported in the literature (Kobayashi & Konishi, 2008; Walgren et al., 1998; Zha, Xu, Wang, & Gu, 2008) with modification. The apical side of the Coco-2 cell monolayer cultured in the Transwell inserts and the basolateral side were washed 3 times with a Hank's balanced salt solution (HBSS; GIBCO) before the test solution was added. To measure the apical-to-basolateral permeability, 0.5 mL of the test solution containing 370 μg/mL sesaminol triglucoside (ST) and 1.5 mL of HBSS were added to the apical and basolateral sides, respectively and then incubated at 37 °C for 0.5, 1, 2 and 4 h. The concentration of ST used was determined according to the results of the Caco-2 cell viability test (data not shown). Prior to starting the experiment, LGSM containing sesaminol triglucoside was dissolved and diluted with HBSS. After incubation for 0.5, 1, 2 and 4 h, apical and basolateral solutions were collected and then the concentration of ST was measured by HPLC.

The apparent permeability coefficient (P_{app} in cm/s) was determined over a time course of 4 h. It was calculated according to the following equation:

$$P_{app} = (V/AC_0) \times (dC/dt)$$

where, V = the volume of solution in the basolateral side (1.5 mL), A = the membrane surface area (1.12 cm^2), C_0 = the initial concentration in the apical side, and dC/dt = the change in concentration in the basolateral side over time.

The transport efficiency (%) is defined as follows:

Transport efficiency (%)
= (Concentration of ST transported in the basolateral side)
/(Initial concentration of ST added to the apical side) × 100.

2.7. Absorption experiments

The absorption study was performed according to methods reported in the literature (Boyer et al., 2004; Yi et al., 2006) with modification. After removing the medium in the apical and basolateral sides, the cell membranes were washed 3 times with HBSS and then removed from the insert. Sesaminol triglucoside was extracted by methanol. Cells were sonicated for 15 min and centrifuged at 2000*g* for 5 min at 4 °C. The methanol supernatant was collected and cells were extracted two more times with 1 mL of methanol, vortexed for 1 min, and centrifuged again at 2000*g* for 5 min at 4 °C. The supernatant was evaporated to dryness under nitrogen and reconstituted in 500 μL of methanol. The extract solutions were then injected into HPLC.

The absorption efficiency (%) is defined as follows:

Absorption efficiency (%)
= (Concentration of ST retained in Caco-2 cells)
/(Initial concentration of ST added to the apical side) × 100.

2.8. HPLC analysis

Concentrations of sesaminol triglucoside on the apical side, the intracellular and the basolateral sides, after transport experiment by Caco-2 cell monolayer model, were determined by HPLC. The HPLC system consisted of a Shimadzu LC-10AT pump (Kyoto, Japan), a Hitachi L-4250 UV detector (Tokyo, Japan), and a Shimadzu SIL-10AF autosampler (Kyoto, Japan). Data acquisition was performed on a SISC programm (Taipei, Taiwan). The Cosmosil 5C18-AR-II column (250 mm × 4.6 mm, and 5 μm pore size, Nacalai Tesque, Kyoto, Japan) was maintained at 25 °C. The detector wavelength was 290 nm. The solvent system used was (A) water (B) methanol. The linear gradient programm used was the following: flow rate = 1.0 mL/min; 0–25 min, (A) 60% and (B) 40%; after 25 min, (A) 0% and (B) 100%. Injection volume was 20 μL.

2.9. Statistical analysis

All data were reported as mean ± standard deviation (SD) for three replicates of each group. Data were analysed by *t*-test analysis of variance, and the differences were considered to be statistically significant at $p < 0.05$.

3. Results and discussion

3.1. Preparation of nano/sub-microsized lignan glycosides from sesame meal

LGSM in this study was the crude extract of lignan glycosides from black sesame meal. For the preparation of LGSM, raw sesame meal was extracted with *n*-hexane (1:10, g/mL) by stirring for 8 h (2 times). After removal of supernatant, the defatted sesame meal was collected and then extracted with 80% methanol (1:10, g/mL) by stirring for 8 h (2 times). This methanol extract was desolventized under reduced pressure to obtain the crude extract of lignan glycosides from sesame meal. The yield of LGSM from raw sesame meal was approximately 6%. LGSM contained 18.5% sesaminol triglucoside, an important bioactive compound in sesame meal. We used wet-milling machine to make LGSM nano/sub-microsuspension. Milling was performed using Yttria-stabilised zirconia balls with a diameter of 0.3 mm, which offered high hardness, fracture toughness and chemical stability (Yu et al., 2006). The crude methanol extract of LGSM (4 g) was suspended in 400 mL of deionised water. Effect of rotation speed (600, 1800 and 3600 rpm) and milling time (5, 10, 30, 60 and 90 min) on size distribution of LGSM suspension was investigated. Effective size reduction could be achieved by strong shear force and high frequency compression during milling. Results showed that smaller particle size and narrower size distribution could be made with rotation speed at

3600 rpm than with 1800 and 600 rpm. The average particle sizes of LGSM after 30 min of milling with a rotation speed of 600, 1800 and 3600 rpm were 315.3 ± 15.5, 217.0 ± 8.2 and 189.0 ± 4.4 nm, respectively. The average particle size of LGSM reduced from around 2 μm to 189 nm after 30 min of milling with a rotation speed of 3600 rpm. Two phases of size reduction were shown during milling (Fig. 2a). During the first 10 min, the particle size reduced dramatically, and then slowly from 10 to 90 min. It might be due to the fact that bigger particles were preferentially milled by zirconium balls in the first 10 min. The number of big particles decreased after the first 10 min so that size reduction was limited after 10 min. Similar trend was found in the literature (Yu et al., 2006). In addition, the efficiency of milling was poor at high solid concentration. Overall, the most effective milling conditions were as followed: 3600 rpm of rotation speed, 30 min of milling time and 1% of solid concentration. LGSM nano/sub-microsuspension could be obtained by the medium grinding technology. This wet-milling technology using Yttria-stabilised zirconia beads as milling media has also been used to produce physically stable red mould rice dispersions having the particle size of 410 nm along with higher monacolin K and lower citrinin extraction yields (Yu et al., 2006). Similarly, ketoconazole nanoparticles were also prepared using a media-milling technique with milling media comprised Yttria-stabilised zirconia beads (Basa, 2008).

3.2. Particle size and morphology determination

The particle size distribution of LGSM before and after media-milling is shown in Fig. 2b and c. N-LGSM had narrow size distribution with one peak. The nano/sub-microsuspension was very homogenous and monodisperse. In addition, the TEM photograph (Fig. 3a) showed that the N-LGSM are nano/sub-microparticles having particle size around 200 nm with spherical and homogeneous morphology. Interestingly, the possible formation of nanoemulsion droplets was found in Fig. 3a. In order to prove the formation of nanoemulsion, Sudan stain test was used to determine if there was a presence of lipids. Sudan III is a dye that selectively stains lipids. The photomicrograph in Fig. 3b showed the positive result of Sudan test. Some droplets were dyed red, indicating the existence of lipid. High-speed homogenisation during wet-milling may cause some extent of nanoemulsion whilst the sample

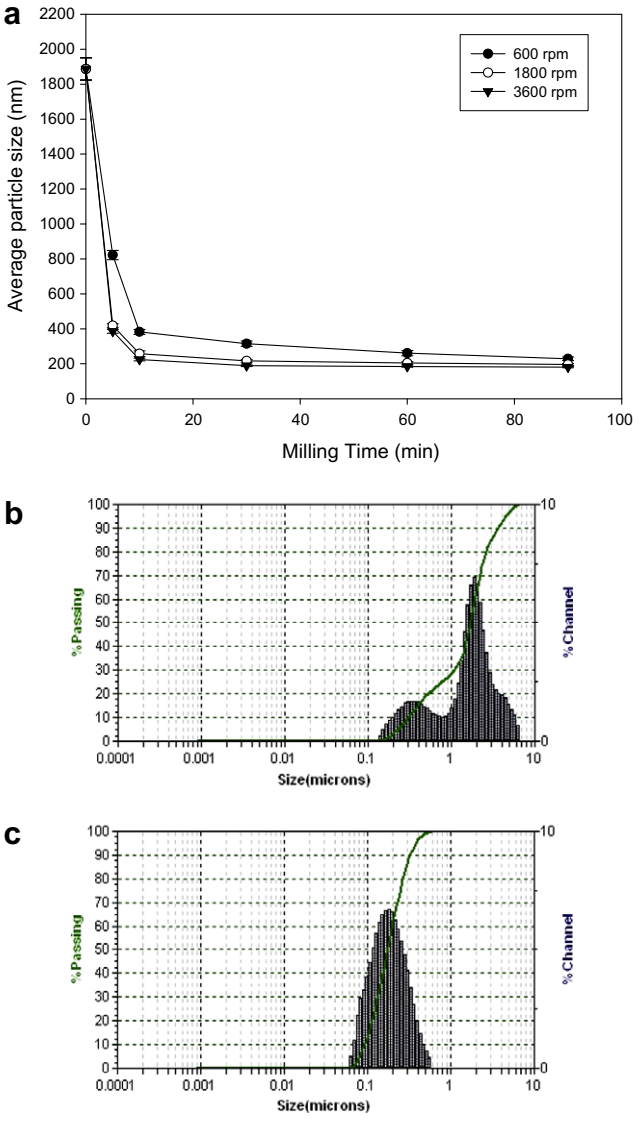

Fig. 2. Average particle size of lignan glycosides from sesame meal (LGSM) by media-milling with different agitation speed and milling time (a). Particle size distribution of LGSM before (b) and after (c) milling process by 0.3 mm grinding media for 30 min at 3600 rpm.

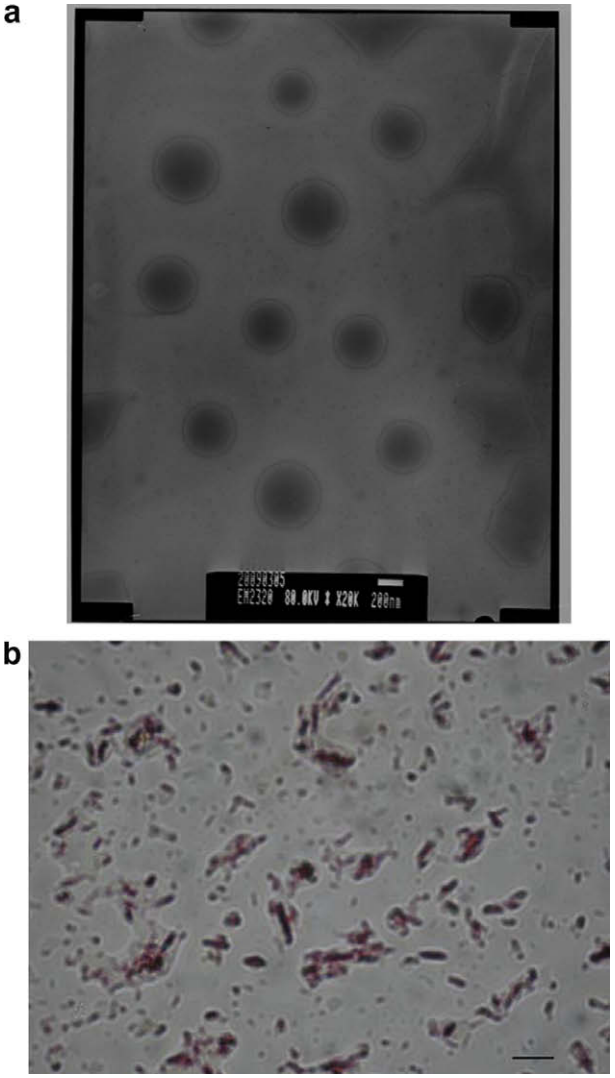

Fig. 3. Transmission electron micrograph (a) and photomicrograph stained by Sudan III (b) of nano/sub-microsized LGSM (N-LGSM). The scale bars in (a) and (b) represents a distance of 200 nm and 2 μm, respectively.

contains lipid and protein. The composition analysis of the sesame meal from Yuan-Shun Food Co. and LGSM was also performed. The results showed that sesame meal contains 5.58 ± 0.05% of moisture, 10.21 ± 0.19% of ash, 23.59 ± 0.09% of crude fat, 25.92 ± 0.50% of crude protein and 34.70% of nitrogen-free extract plus crude fibre. LGSM, the extracts of sesame meal, contained 5.50 ± 0.45% of moisture, 5.46 ± 0.03% of ash, 10.51 ± 0.16% of crude fat, 15.78 ± 0.67% of crude protein and 62.75% of nitrogen-free extract plus crude fibre. Overall, the possible formation of nanoemulsion droplets maybe due to high lipid and protein content, and the high-speed homogenisation during the process of nanonization.

3.3. Transport of ST across Caco-2 cell monolayer

A method of measuring ST, the main component in lignan glycosides from sesame meal, was developed in this study. The determination of ST was performed using HPLC/UV for quantification. The method has been used to analyse ST on the apical side, the intracellular and the basolateral side, after transport experiment by Caco-2 cell monolayer model. The maximum absorption wavelength (290 nm) of ST was determined by a photodioarray detector, it was employed as the UV detecting wavelength in the following analysis. The linear gradient programm of mixed solvents of water and methanol was used. The Cosmosil 5C18-AR-II column showed good performance in HPLC chromatograms. The retention time of ST peak was 11.8 min (Fig. 4a). This rapid and reliable analytical method was used in the following experiments.

After 4 h of experiment, most of ST still remained on the apical side, indicating that most ST did not cross Caco-2 cell monolayer to the basolateral side. HPLC chromatograms of ST on the apical side, intracellular and basolateral side after 4 h of transport experiment are shown in Fig. 4b–d. Much bigger peak area of ST was found on apical side compared to basolateral side and in Caco-2 cells. Distribution (%) of ST on apical side, intracellular and basolateral side after 4 h incubation with Caco-2 cells were 97.59, 0.19 and 1.52, respectively. In the time course study, concentrations of ST in both LGSM and N-LGSM transported across Caco-2 cell monolayer were increased with the prolongation of time. The transport was time-dependent and size-dependent. At each time point, the concentration of ST in N-LGSM detected on basolateral side was higher than that in LGSM. In LGSM group, distribution (%) of ST on basolateral side at 0.5, 1, 2 and 4 h were 0.39 ± 0.05, 0.68 ± 0.12, 1.04 ± 0.19 and 1.15 ± 0.22, respectively. In N-LGSM group, distribution (%) of ST on basolateral side at 0.5, 1, 2 and 4 h were 0.64 ± 0.11, 1.01 ± 0.16, 1.45 ± 0.25 and 1.52 ± 0.17, respectively, significantly higher than those in LGSM group ($p < 0.05$). The study of pure ST across Caco-2 cell monolayer was also investigated. Distribution (%) of ST on basolateral side at 0.5, 1, 2 and 4 h were 0.51 ± 0.09, 0.86 ± 0.17, 1.17 ± 0.10 and 1.32 ± 0.08, respectively.

The increase of transport efficiencies of ST in N-LGSM compared to those in LGSM at 0.5, 1, 2 and 4 h were 64.10, 48.53, 39.42 and 32.20%, respectively (Table 1). It showed that nanonization made ST easier and faster to transport across Caco-2 cell monolayer, especially in the beginning of the time course study. Higher transport efficiencies of ST in N-LGSM compared to those in pure ST group were also found. The increase percentages at 0.5, 1, 2 and 4 h were 25.49, 17.44, 23.93 and 15.15%, respectively.

The permeability results also showed that ST in N-LGSM was better transported across Caco-2 cell monolayer than that in LGSM. The permeabilities of ST in pure ST, LGSM and N-LGSM groups were 1.23×10^{-6}, 1.07×10^{-6} and 1.41×10^{-6} (cm/s), respectively, indicating ST in N-LGSM was more efficiently transported. After completion of transport experiment, the TEER values were

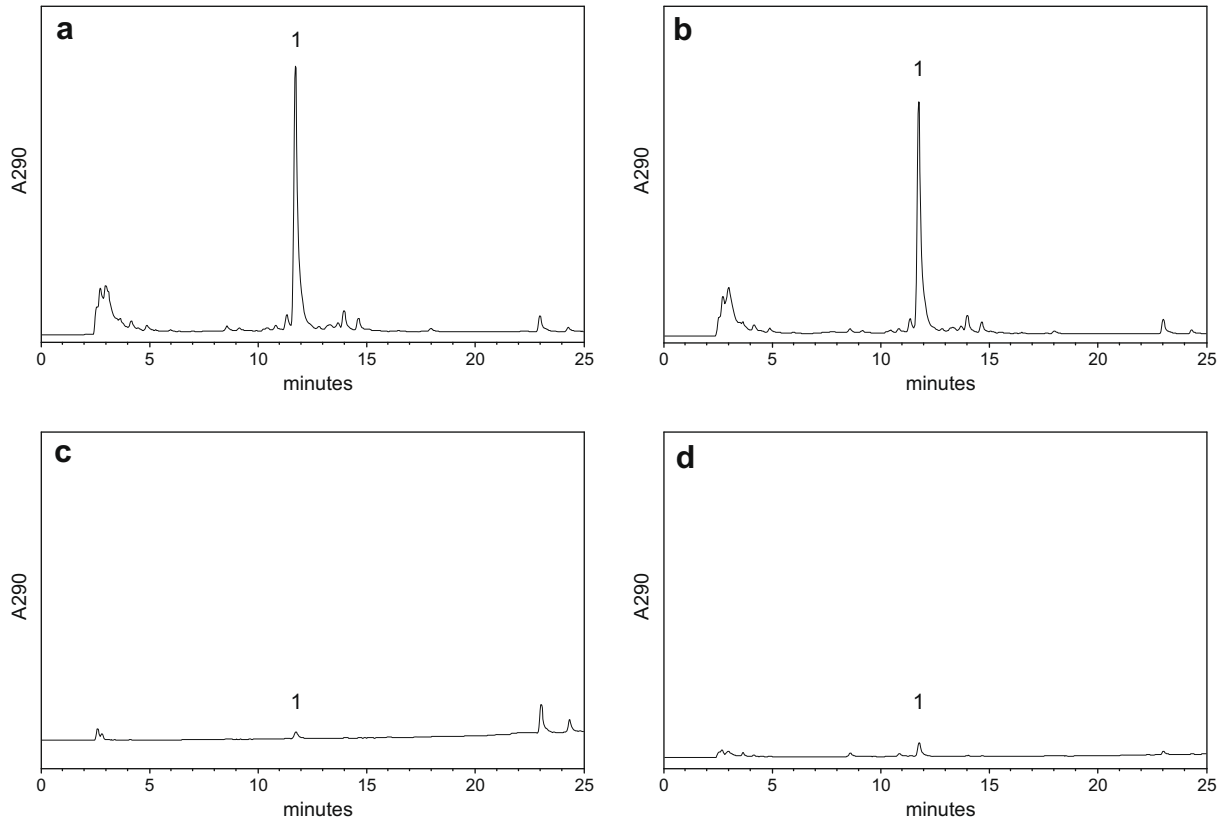

Fig. 4. Typical HPLC chromatogram of lignan glycosides from sesame meal containing 370 μg/mL of sesaminol triglucoside (a). HPLC chromatograms of sesaminol triglucoside on apical side (b), intracellular (c) and basolateral side (d) after 4 h incubation with Caco-2 cells (N-LGSM group, added concentration of 370 μg/mL). 1: Sesaminol triglucoside.

Table 1
Transport efficiency (%) of sesaminol triglucoside (ST) in LGSM and N-LGSM groups across Caco-2 cell monolayer from apical to basolateral side.

Time (h)	Transport efficiency (%)		
	Pure ST	LGSM	N-LGSM
0.5	0.51 ± 0.09	0.39 ± 0.05	0.64 ± 0.11 (25.49%[a], 64.10%[b])
1	0.86 ± 0.17	0.68 ± 0.12	1.01 ± 0.16 (17.44%[a], 48.53%[b])
2	1.17 ± 0.10	1.04 ± 0.19	1.45 ± 0.25 ([a]23.93%, 39.42%[b])
4	1.32 ± 0.08	1.15 ± 0.22	1.52 ± 0.17 (15.15%[a], 32.20%[b])

N-LGSM: Nano/sub-microsized LGSM. Data expressed as average of three independent experiments. In each experiment, three inserts were used at each time point of each group. Added concentration of ST in pure ST, LGSM and N-LGSM groups was 370 μg/mL. Transport efficiency (%) = (ST concentration on basolateral side)/(initial ST concentration loaded on apical side) × 100.

[a] Increase of transport efficiency in N-LGSM compared to pure ST (%) = (ST concentration in N-LGSM − ST concentration in pure ST)/(ST concentration in pure ST) × 100.

[b] Increase of transport efficiency in N-LGSM compared to LGSM (%) = (ST concentration in N-LGSM − ST concentration in LGSM)/(ST concentration in LGSM) × 100.

Table 2
Absorption efficiency (%) of sesaminol triglucoside (ST) in LGSM and N-LGSM groups by Caco-2 cells.

Time (h)	Absorption efficiency (%)		
	Pure ST	LGSM	N-LGSM
0.5	0.06 ± 0.03	0.06 ± 0.02	0.08 ± 0.02 (33.30%[a], 33.30%[b])
1	0.12 ± 0.01	0.10 ± 0.05	0.13 ± 0.02 (8.33%[a], 30.00%[b])
2	0.15 ± 0.02	0.13 ± 0.03	0.17 ± 0.03 (13.33%[a], 30.80%[b])
4	0.16 ± 0.02	0.14 ± 0.03	0.19 ± 0.03 (18.75%[a], 35.70%[b])

N-LGSM: Nano/sub-microsized LGSM. Data expressed as average of three independent experiments. In each experiment, three inserts were used at each time point of each group. Added concentration of ST in pure ST, LGSM and N-LGSM groups was 370 μg/mL. Absorption efficiency (%) = (ST concentration of Caco-2 cell extract) − (initial ST concentration loaded on apical side) × 100.

[a] Increase of absorption efficiency in N-LGSM compared to pure ST (%) = (ST concentration in N-LGSM − ST concentration in pure ST)/(ST concentration in pure ST) × 100.

[b] Increase of absorption efficiency in N-LGSM compared to LGSM (%) = (ST concentration in N-LGSM − ST concentration in LGSM)/(ST concentration in LGSM) × 100.

also examined. The TEER values were unchanged after the experiment, indicating added ST had no negative effect on the Caco-2 cell monolayer. Similar results had also been reported. Permeability of nanoparticle 301029, an inhibitor of bovine viral diarrhaea virus, across the Caco-2 monolayer was about four times higher than that of microparticle 301029 (Jia et al., 2002). Chromium nanoparticle exhibits higher permeability than chromium picolinate and chromium chloride across the Caco-2 monolayer (Zha et al., 2008). Szentkuti (1997) found that the smaller the particle, the faster the penetration action across the mucus barrier. Latex nanoparticles (14 and 415 nm) could penetrate the mucus gel layer in 2 and 30 min, respectively.

Good correlations existed between Caco-2 permeability and fraction of drug absorbed after oral administrations were shown in several studies. Summary of *in vitro* permeability across Caco-2 monolayer and *in vivo* oral bioavailability in rats or human was reported (Foger et al., 2007). A good correlation between the two systems was found. In addition, Yee (1997) reported that *in vitro* permeability across Caco-2 cells can predict *in vivo* absorption in man. A strong correlation was observed between *in vivo* human absorption and *in vitro* P_{app} for a variety of compounds ($R^2 = 0.95$, $N = 35$). According to the literature, compounds with a very low Caco-2 cell permeability (P_{app} less than 3×10^{-6} cm/s) exhibited poor oral absorption, whereas compounds with a high P_{app} had excellent oral absorption (Lau et al., 2004). The present permeability result showed that the P_{app} of LGSM was only 1.07×10^{-6} (cm/s), indicating ST is a poor oral absorbed compound.

3.4. Absorption of ST by Caco-2 cells

The absorption of ST by Caco-2 cells was time-dependent and size-dependent. In the time course study, ST concentrations of LGSM and N-LGSM in Caco-2 cells were increased with the prolongation of time. At each time point, the concentration of ST in N-LGSM was higher than that in LGSM. The absorption efficiencies at 0.5, 1, 2 and 4 h were 0.06, 0.10, 0.13 and 0.14% for LGSM, whereas 0.08, 0.13, 0.17 and 0.19% for N-LGSM (Table 2). This showed that ST is a compound with quite low bioavailability. The increase percentages of absorption efficiencies of ST in N-LGSM compared to those in pure ST and LGSM at each time point were 8.33–33.30% and 30.00–35.70%, respectively. N-LGSM exhibited higher absorption efficiencies than LGSM in Caco-2 cells. Although the absolute absorption efficiency of LGSM is low, over 30% in relative absorption efficiency between LGSM and N-LGSM is quite significant. Previous reports showed that the uptake of nanoparticles was size-dependent (Desai, Labhasetwar, Amidon, & Levy, 1996; Desai, Labhasetwar, Walter, Levy, & Amidon, 1997). The authors explained that it might be due to efficient interfacial interaction of nanoparticles with cell membrane compared to larger diameter microparticles.

The particle sizes of LGSM and N-LGSM were 2 μm and 189 nm, respectively, indicating at least 100-fold higher surface area of N-LGSM compared to LGSM. The higher absorption efficiency of LGSM after nano/sub-microsizing might be due to its smaller particle size and much larger surface area. An increase in adhesion surface area between nanoparticles and the mucin layer coating intestinal epithelium of villi facilitates the nanosized drug to traverse the mucin layer and the epithelial cells (Jia et al., 2002). Jia et al. (2003) used rats to evaluate the pharmacokinetic profiles of carbendazim, a novel anticancer drug. The bioavailability of regular carbendazim (7 μm) and its nanoparticle (280 nm) made by wet-milling were compared. It was found that the relative bioavailability of nanoparticle carbendazim versus regular carbendazim was 166%. One explanation for the high uptake efficiency of smaller diameter nanoparticles is owing to the more efficient interfacial interaction with the cell membrane compared with larger diameter microparticles.

It is interesting to find that the absorption efficiencies were in the order N-LGSM > pure ST > LGSM. The higher absorption efficiencies of ST in N-LGSM than those of pure ST might be attributed to the possible formation of nanoemulsion droplets during the process of nanonization. In the present investigations, possible LGSM nanoemulsion droplets were found in the TEM photograph. Nanoemulsion formulation can enhance the bioavailability of drugs as reported in the literatures. The relative bioavailability of ramipril nanoemulsion to that of conventional capsule form was found to be 229.62% whereas to that of drug suspension was 539.49% in rats (Shafiq et al., 2007). Coenzyme Q_{10} (CoQ_{10}) nanosized emulsion (60 nm) exhibited 1.7-fold higher AUC and C_{max} than CoQ_{10} crystal suspension in pharmacokinetic study (Hatanaka, Jimura, Lai-Fu, Onoue, & Yamada, 2008). The better performance of N-LGSM in this study may be due to the formation of nanoemulsion droplets.

The permeability and absorption efficiency of compounds might be lower in the Caco-2 cell monolayer model than in the animal and human model. Compared to *in vivo* models, Caco-2 cell lacks entero-hepatic circulation and the phase I metabolic enzymes, such as CYP3A4 (Lau et al., 2004). Lennernas (1998) reported that the lower permeability in Caco-2 monolayer might be due to lower paracellular and larger area available in humans, as it is assumed that the absorption of hydrophilic compounds is so slow that a larger surface area of the intervillous space is exposed. In addition,

TEER of Caco-2 cell monolayer is much higher than that of intestines in rats and human. In our previous findings from pharmacokinetic study in rats, the oral bioavailability of LGSM and N-LGSM were 0.18% and 0.26%, respectively, which corresponded to the present Caco-2 cell results (0.14% and 0.19% for LGSM and N-LGSM). We also found that absorption efficiency of ST was lower in the Caco-2 cell monolayer model than in the rat model.

4. Conclusions

N-LGSM showed 30.0 to 64.1% higher transport and absorption efficiency than LGSM at each time point in Caco-2 cell monolayer model. It seems that nanonization may be a useful way to enhance the efficiency of intestinal absorption and bioavailability of sesaminol triglucoside. The superior performance of nano/sub-microsized LGSM may be attributed to the following factors: (a) smaller particle size and larger surface area provided by the fine particles approximately 200 nm; (b) increased mucosal permeability, and (c) improved intestinal absorption due to the formation of nano-emulsion droplets. In order to fully understand the possible difference between LGSM and N-LGSM *in vivo*, further investigations are needed on the absorption, distribution, metabolism and excretion in rats.

Acknowledgements

We thank Dr. Kaeko Murota, The University of Tokushima, Japan, for her technical advice. This study was supported by a research grant, DOH97-TD-F-113 from the Department of Health, Taiwan.

References

Artursson, P. (1990). Epithelial transport of drugs in cell culture. I: A model for studying the passive diffusion of drugs over intestinal absorptive (Caco-2) cells. *Journal of Pharmaceutical Sciences, 79*, 476–482.

Basa, S. (2008). Production and in vitro characterization of solid dosage form incorporating drug nanoparticles. *Drug Development and Industrial Pharmacy, 7*, 1–10.

Boyer, J., Brown, D., & Liu, R. H. (2004). Uptake of quercetin and quercetin 3-glucoside from whole onion and apple peel extracts by Caco-2 cell monolayers. *Journal of Agricultural and Food Chemistry, 52*, 7172–7179.

Desai, M. P., Labhasetwar, V., Amidon, G. L., & Levy, R. J. (1996). Gastrointestinal uptake of biodegradable microparticles: Effect of particle size. *Pharmaceutical Research, 12*, 1838–1845.

Desai, M. P., Labhasetwar, V., Walter, E., Levy, R. J., & Amidon, G. L. (1997). The mechanism of uptake of biodegradable microparticles in Caco-2 cells is size dependent. *Pharmaceutical Research, 14*, 1568–1573.

Foger, F., Kopf, A., Loretz, B., Albrecht, K., & Bernkop-Schnurch, A. (2007). Correlation of in vitro and in vivo models for the oral absorption of peptide drugs. *Amino acids, 35*, 233–241.

Gao, L., Zhang, D., Chen, M., Duan, C., Dai, W., Jia, L., et al. (2008). Studies on pharmacokinetics and tissue distribution of oridonin nanosuspensions. *International Journal of Pharmaceutics, 355*, 321–327.

Hatanaka, J., Jimura, Y., Lai-Fu, Z., Onoue, S., & Yamada, S. (2008). Physicochemical and pharmacokinetic characterization of water-soluble Coenzyme Q_{10} formulations. *International Journal of Pharmaceutics, 363*, 112–117.

Jia, L., Wong, H., Cerna, C., & Weitman, S. D. (2002). Effect of nanonization on absorption of 301029: Ex vivo and in vivo pharmacokinetic correlations determined by liquid chromatography/mass spectrometry. *Pharmaceutical Research, 19*, 1092–1096.

Jia, L., Wong, H., Wang, Y., Garza, M., & Weitman, S. D. (2003). Carbendazim: Disposition, cellular permeability, metabolite identification, and pharmacokinetic comparison with its nanoparticle. *Journal of Pharmaceutical Science, 92*, 161–172.

Kang, M. H., Kawai, Y., Naito, M., & Osawa, T. (1999). Dietary defatted sesame flour decreases susceptibility to oxidative stress in hypercholesterolemic rabbits. *Journal of Nutrition, 129*, 1885–1890.

Katsuzaki, H., Kawakishi, S., & Osawa, T. (1994). Sesaminol glucosides in sesame seeds. *Phytochemistry, 35*, 773–776.

Kobayashi, S., & Konishi, Y. (2008). Transepithelial transport of flavone in intestinal Caco-2 cell monolayers. *Biochemical and Biophysical Research Communications, 368*, 23–29.

Lau, Y. Y., Chen, Y. H., Liu, T. T., Li, C., Cui, X., White, R. E., et al. (2004). Evaluation of a novel in vitro Caco-2 hepatocyte hybrid system for predicting in vivo oral bioavailability. *Drug Metabolism and Disposition, 32*, 937–942.

Lee, S. Y., Ha, T. Y., Son, D. J., Kim, S. R., & Hong, J. T. (2005). Effect of sesaminol glucosides on β-amyloid-induced PC 12 cell death through antioxidant mechanisms. *Neuroscience Research, 52*, 330–341.

Lennernas, H. (1998). Human intestinal permeability. *Journal of Pharmaceutical Science, 87*, 403–410.

Namiki, M. (1995). The chemistry and physiological functions of sesame. *Food Research International, 11*, 281–329.

Shafiq, S., Shakeel, F., Talegaonkar, S., Ahmad, F. J., Khar, R. K., Ali, M., et al. (2007). Development and bioavailability assessment of ramipril nanoemulsion formulation. *European Journal of Pharmaceutics and Biopharmaceutics, 66*, 227–243.

Sheng, H. Q., Hirose, Y., Hata, K., Zheng, Q., Kuno, T., Asano, N., et al. (2007). Modifying effect of dietary sesaminol glucosides on the formation of azoxymethane-induced premalignant lesions of rat colon. *Cancer Letter, 246*, 63–68.

Shyu, Y. S., & Hwang, L. S. (2002). Antioxidative activity of the crude extract of lignan glycosides from unroasted Burma black sesame meal. *Food Research International, 236*, 357–365.

Szentkuti, L. (1997). Light microscopical observations on luminally administered dyes, dextrans, nanospheres and microspheres in the pre-epithelial mucus gel layer of the rat distal colon. *Journal of Control Release, 46*, 233–242.

Walgren, R. A., Walle, U. K., & Walle, T. (1998). Transport of quercetin and its glucosides across human intestinal epithelial Caco-2 cells. *Biochemical Pharmacology, 55*, 1721–1727.

Yee, S. (1997). In vitro permeability across Caco-2 cells (colonic) can predict in vivo (small intestinal) absorption in man – Fact or myth. *Pharmaceutical Research, 14*, 763–766.

Yi, W., Akoh, C. C., Fischer, J., & Krewer, G. (2006). Absorption of anthocyanins from blueberry extracts by Caco-2 human intestinal cell monolayers. *Journal of Agricultural and Food Chemistry, 54*, 5651–5658.

Yu, C. C., Lee, C. L., & Pan, T. M. (2006). A novel formulation approach for preparation of nanoparticulate red mold rice. *Journal of Agricultural and Food Chemistry, 54*, 6845–6851.

Zha, L. Y., Xu, Z. R., Wang, M. Q., & Gu, L. Y. (2008). Chromium nanoparticle exhibits higher absorption efficiency than chromium picolinate and chromium chloride in Caco-2 cell monolayers. *Journal of Animal Physiology and Animal Nutrition, 92*, 131–140.